

Research article

Open Access

Chemical and biomechanical characterization of hyperhomocysteinemic bone disease in an animal model

Priscilla G Massé¹, Adele L Boskey², Israel Ziv³, Peter Hauschka⁴, Sharon M Donovan⁵, David S Howell⁶ and David EC Cole*⁷

Address: ¹School of Nutrition, University of Moncton, Moncton NB E1A 3E9, Canada, ²Hospital for Special Surgery, and Weill Medical College of Cornell University, New York NY 10021, USA, ³Dept of Orthopaedic Surgery, School of Medicine & Biomechanics, State University of New York, Buffalo NY 14214, USA, ⁴Massachusetts Children's Hospital and Harvard University, Boston MA 02115, USA, ⁵Division of Food Science and Human Nutrition, University of Illinois, Urbana IL 46835, USA, ⁶VA Medical Center and University of Miami School of Medicine, Miami, FL 33101, USA and ⁷Depts. of Laboratory Medicine & Pathobiology, Medicine, and Pediatrics (Genetics), University of Toronto, Toronto ON M5G 1L5, Canada

Email: Priscilla G Massé - massep@umoncton.ca; Adele L Boskey - boskeya@hss.edu; Israel Ziv - israelz@buffalo.edu; Peter Hauschka - hauschka@hub.tch.harvard.edu; Sharon M Donovan - sdonovan@uiuc.edu; David S Howell - gjackson@med.miami.edu; David EC Cole* - davidec.cole@utoronto.ca

* Corresponding author

Published: 20 February 2003

Received: 30 November 2002

BMC Musculoskeletal Disorders 2003, 4:2

Accepted: 20 February 2003

This article is available from: <http://www.biomedcentral.com/1471-2474/4/2>

© 2003 Massé et al; licensee BioMed Central Ltd. This is an Open Access article: verbatim copying and redistribution of this article are permitted in all media for any purpose, provided this notice is preserved along with the article's original URL.

Abstract

Background: Classical homocystinuria is an autosomal recessive disorder caused by cystathionine β -synthase (CBS) deficiency and characterized by distinctive alterations of bone growth and skeletal development. Skeletal changes include a reduction in bone density, making it a potentially attractive model for the study of idiopathic osteoporosis.

Methods: To investigate this aspect of hyperhomocysteinemia, we supplemented developing chicks ($n = 8$) with 0.6% dl-homocysteine (hCySH) for the first 8 weeks of life in comparison to controls ($n = 10$), and studied biochemical, biomechanical and morphologic effects of this nutritional intervention.

Results: hCySH-fed animals grew faster and had longer tibiae at the end of the study. Plasma levels of hCySH, methionine, cystathionine, and inorganic sulfate were higher, but calcium, phosphate, and other indices of osteoblast metabolism were not different. Radiographs of the lower limbs showed generalized osteopenia and accelerated epiphyseal ossification with distinct metaphyseal and suprametaphyseal lucencies similar to those found in human homocystinurics. Although biomechanical testing of the tibiae, including maximal load to failure and bone stiffness, indicated stronger bone, strength was proportional to the increased length and cortical thickness in the hCySH-supplemented group. Bone ash weights and IR-spectroscopy of cortical bone showed no difference in mineral content, but there were higher $\text{Ca}^{2+}/\text{PO}_4^{3-}$ and lower $\text{Ca}^{2+}/\text{CO}_3^{2-}$ molar ratios than in controls. Mineral crystallization was unchanged.

Conclusion: In this chick model, hyperhomocysteinemia causes greater radial and longitudinal bone growth, despite normal indices of bone formation. Although there is also evidence for an abnormal matrix and altered bone composition, our finding of normal biomechanical bone strength, once corrected for altered morphometry, suggests that any increase in the risk of long bone fracture in human hyperhomocysteinemic disease is small. We also conclude that the hCySH-supplemented chick is a promising model for study of the connective tissue abnormalities associated with homocystinuria and an important alternative model to the CBS knock-out mouse.

Background

Classical homocystinuria is an inborn error of sulfur amino acid metabolism caused by cystathionine β -synthase (CBS) deficiency [1]. The excess homocysteine (hCySH) that accumulates because of this defect is exported into the circulation and spills into the urine. In humans, CBS deficiency manifests as a distinctive spondylo-epimeta-physeal dysplasia, characterized by accelerated skeletal growth, osteopenia, elongated appendicular skeleton and flattening of the vertebral bodies [2,3]. The overall risk of osteoporosis has been reported to be 50% by age 16 [4], and bone mineral density measured by dual X-ray absorptiometry is reduced in affected children [5]. However, there are no good estimates of the frequency or severity of fractures, and interactions with late-onset physiologic bone loss have not been reported. Some of the osseous manifestations are attributable to a disturbance in collagen cross-links, but there is still little known about the molecular mechanisms generating the dysmorphic skeletal phenotype [6], and the CBS-deficient knock-out mouse offers few clues. [7]. The role of intermolecular collagen cross-links in bone has been adduced in part from studies of lathyrism caused by the compound, β -amino-propionitrile (BAPN), found in the sweet pea (*Lathyrus odoratus*). BAPN irreversibly inhibits lysyl oxidase, and blocks initial collagen cross-link formation [8,9].

The fast-growing chick has been introduced as an animal model for detailed study of soft connective tissue abnormalities resulting from controlled perturbations of the transsulfuration pathway [10–12]. In animals receiving aminoacetonitrile, a less toxic analog of BAPN, electron microscopy of long bones shows significant enlargement of Type I collagen fibrils while a similar but less severe abnormality is observed in vitamin B₆-deficiency and in hyperhomocysteinemia induced by hCySH added to the diet [13]. Changes in collagen solubility and collagen cross-linking are hallmarks of connective tissue changes associated with these dietary manipulations [14–16].

The mechanical integrity of bone is dependent on both collagenous matrix (which allows for plastic deformation of the tissue) and mineral (which allows for the elastic deformation) [17]. Lathyrism induced by BAPN affects both components of bone [18–21]. In our hands, vitamin B₆ deficiency has been a useful alternative model to study the effect(s) of altered intermolecular collagen cross-links on whole bone, because the mineral component is unaltered [15]. In growing chicks fed a B₆-deficient diet, there were no changes in bone length, bone diameter, or moment of inertia, but mechanical performance was altered. Moreover, histomorphometric and radiological studies showed low-turnover osteopenia [14].

Table 1: Basal diet¹

Constituents	Composition (w/w %)
Soyamin	23.40
Corn	33.00
Cerelose (glucose monohydrate)	28.00
Corn Oil	4.90
Mineral salts ²	5.35
Vitamins ³	2.00
Trace minerals ⁴	2.00
l-methionine	0.30
dl-homocysteine	0.60
Glycine	0.30
Choline chloride	0.15

¹ Metabolizable energy calculated as 13.8 MJ (3000 kcal) per kg diet ² Salt mixture (g/kg diet): CaHPO₄, 20.0; CaCO₃, 15.0; KH₂PO₄, 11.0; NaCl, 4; MgSO₄, 3.5. ³ Vitamin premix (mg/kg diet): retinyl palmitate, 5.49; cholecalciferol, 0.016; all-rac- α -tocopheryl acetate, 55.0; menadione sodium bisulfite, 1.52; thiamine • HCl, 15; nicotinic acid, 50; pyridoxine • HCl, 3; calcium-d-pantothenate, 20; cyanocobalamin, 0.02; folic acid, 6.0; biotin, 0.6. ⁴ Trace minerals (mg/kg diet): C₁₂H₂₂FeO₄ • 2H₂O, 700; MnSO₄ • 7H₂O, 170; ZnO, 65; CuSO₄ • 5H₂O, 20; Na₂MoO₄ • 2H₂O, 5; CoCl₂ • 6H₂O, 1.5; Na₂SeO₃ • 5H₂O, 0.5; KIO₃, 0.7.

The objectives of the present study were to investigate the radiologic, biochemical, and biomechanical properties of bone in the growing chick made hyperhomocysteinemic by excess dietary hCySH and to evaluate those changes in relation to skeletal abnormalities characterizing human CBS-deficiency homocystinuria.

Methods

Animals and diets

Male day-old broiler chicks purchased from the Miami International Hatchery (Miami FL) were randomly assigned to control (n = 10) or experimental (n = 8) groups. They were fed normal diet and diet supplemented with 0.6 % w/w of dl-homocysteine, respectively, over eight weeks. Both diets were supplied by ICN Pharmaceuticals (Aurora, OH) and were identical in terms of protein and essential amino acid content. Both were also identically supplemented with vitamins and minerals to fulfill all nutritional requirements, including specific needs for vitamin B₆, a coenzyme in the transsulfuration pathway, and menadione (vitamin K), which is essential for the synthesis of osteocalcin, involved in bone formation (Table 1). The vitamin D intake was kept constant and the Ca:P molar ratio optimal for chick bone growth was identical in each diet. The dl-hCySH supplement (98% pure) was obtained from Sigma (St. Louis MO).

The animals were kept in a temperature-controlled environment and fed *ad libitum* and a 12 hr constant light cycle was maintained. Chicks were weighed at the beginning of

the experiment, and then on a weekly basis, and the growth curve was used to monitor the health status throughout the experiment. Experimental procedures were reviewed and approved by the research animal care committee of VA Medical Center, Miami FL, in accordance with current National Institutes of Health policies.

Blood biochemistry

At the end of the eight week experiment, samples of fasting blood were collected by jugular venipuncture using heparin or EDTA. The blood was centrifuged and plasma collected for analysis. Erythrocytes were resuspended in an equal volume of isotonic saline and centrifuged. The heparin supernatant was discarded and the erythrocytes analyzed for pyridoxal-5'-phosphate (PLP) according to the methods of Mahuren and Coburn [22]. HPLC with pulsed integrated amperometry was used to measure total hCySH, methionine, cystathionine, and glutathione, as previously described [23].

Plasma free inorganic sulfate was measured by microassay using controlled-flow anion chromatography [24,25]. Plasma calcium, phosphate and bone alkaline phosphatase (ALP: orthophosphoric monoester phosphohydrolase, alkaline EC 3.1.3.1) were assayed on an automated COBAS-BIO autoanalyser (Hoffmann LaRoche, Switzerland). Plasma ALP bone isoenzyme was determined by using bromotetramisole as inhibitor [26]. Plasma osteocalcin, an index of bone formation, was measured in serially diluted samples of plasma by radioimmunoassay [27,28] Circulating IGF-1 level was measured by radioimmunoassay, as described by Zhao et al. [29].

Bone measurements, radiographic evaluation, and mechanical testing

The chick tibiotarsus bone (the tibia) was selected for further analysis because it is known to be the most rapidly growing and, by inference, the bone most susceptible to mechanical stress [30]. Immediately after sacrifice by cervical dislocation, left tibias were dissected, cleaned of soft tissue, wrapped in saline-soaked gauze, and stored at -70°C until testing. Radiographic and biomechanical studies were followed by chemical analyses of mineral and collagen composition.

Whole bones were thawed after 10–20 days of storage (a procedure known not to affect bone biomechanical properties) and maintained in a wet condition while they were weighed and their length measured. They were then immediately tested with 3-point bending, anterior cortex on the tensile side with the 3-point contact centered on the mid-shaft of the bone [31–34]. These tests were performed in ambient air on an MTS closed-loop servohydraulic apparatus at a displacement rate of 6.25 mm/sec.

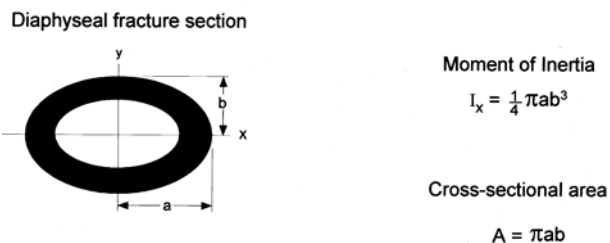


Figure 1
Representation of the fracture section at tibial mid-shaft Inner endosteal and outer periosteal AP (antero-posterior) and ML (medio-lateral) diameters on Y and X axes, respectively. Equations are given for diaphyseal geometries: the moment of inertia (I_x), and the cross-sectional area (A).

Testing to failure was performed in the medio-lateral plane, using an outer support span of 33 mm and an inner span of 11 mm. Load versus displacement of the loading ram was recorded on computer. Specimens were selected randomly for testing and were kept wet with distilled water throughout testing. The whole bone properties of fracture load were determined directly from the load vs. displacement curve for each specimen. Prior to failure testing, each specimen was loaded elastically to 5.62 N at a constant rate of 2.81 N/sec until fracture. Tibias were radiographed (60 kV, 4.5 min) before and after fracture in the anterior-posterior (AP) and medial-lateral (ML) planes.

Typical load/deflection curves with both the elastic (linear) and plastic components separated by the yielding point as described by Burstein et al. [17] were obtained, enabling graphic determination of the following mechanical properties: maximal load, bone stiffness, and energy at failure. To consider the influence of diaphyseal geometrical variation on whole bone mechanical properties, inner endosteal and outer periosteal AP and ML diameters on X and Y axes, respectively, of the tibial fracture section were measured from the radiograph by digital caliper. Two geometric characteristics – moment of inertia of the cross-section in relation to the horizontal axis (I_x) and cross-sectional area (A) – were calculated as shown in Figure 1. Moment of inertia is an indicator of the architectural efficiency of the tibial cross-sectional design [33].

Bone evaluation: mineral and matrix composition

Following mechanical testing, bone samples from the fracture site were lyophilized, ground in a Spex freezer mill (Metuchen, NJ) at liquid nitrogen temperature, and three sets of aliquots set aside for mineral analyses. For analysis of mineral content, triplicate aliquots of 2 to 4 mg

each were transferred to weighed dry crucibles. Dry weight was determined following heating to constant weight at 110°C. Ash weight was determined following heating to constant weight at 600°C. Mineral content was calculated as the ratio of ash weight to dry weight. The ash was dissolved in 1 N HCl, as described for our vitamin B₆ deficiency model [15]. To calculate the Ca²⁺/PO₄³⁻ ratio, the calcium content was measured by atomic absorption spectrophotometry and the phosphate concentration determined spectrophotometrically.

Aliquots of ground bone obtained near the fracture site were also subjected to wide-angle X-ray diffraction using CuK- α radiation. The line width at half-maximum of the c-axis 002 reflection was measured as an index of crystal-line size and perfection [35]. Each assay was repeated in triplicate. Two milligram aliquots of ground bone were mixed with 200 mg KBr, and pellets prepared for infrared spectroscopy. The pellets were analysed at 4 cm⁻¹ resolution on a Mattson Cygnus Fourier Transform Infrared (FT-IR) spectrometer. The spectra were analyzed to provide information on the relative mineral to matrix ratio; that is, the ratio of integrated areas of the phosphate ν_1 , ν_3 mode (900–1200 cm⁻¹) to the amide I band (1580–1650 cm⁻¹) and the carbonate (840–890 cm⁻¹) to phosphate (900–1200 cm⁻¹) ratio [15].

An additional bone sample was dissected from the diaphyseal section, ground as described above, and aliquots used for analysis of hydroxyproline to estimate collagen content [36]. Hydroxyproline analysis was performed on HCl hydrolysates (6 N, 18 h, 110°C) of EDTA-demineralized ground bone.

Data presentation and statistical analysis

Data are reported as mean \pm standard deviation (SD) for 8 experimental and 10 control animals. Differences between groups for biochemical data and biological, chemical and biomechanical parameters of bone were assessed by unpaired Student *t*-test, or non-parametric Mann-Whitney test when data displayed a significantly non-Gaussian distribution. The Bartlett test was used to exclude heteroscedasticity. The two-tailed significance level was set at 0.05. Analysis of covariance was used for bone biomechanical data to adjust for statistical differences in biological variables.

Results

Charted body weights of experimental and control chicks from day 1 to 8 week-old are shown in Figure 2. Mean weights of hCySH-fed chicks increased at a faster rate than in the controls, and were significantly ($P < 0.01$) greater at the end of the experiment. Tibial weights in animals fed a hCySH-rich diet were proportionally (12%) greater compared to controls, but the difference did not reach a signif-

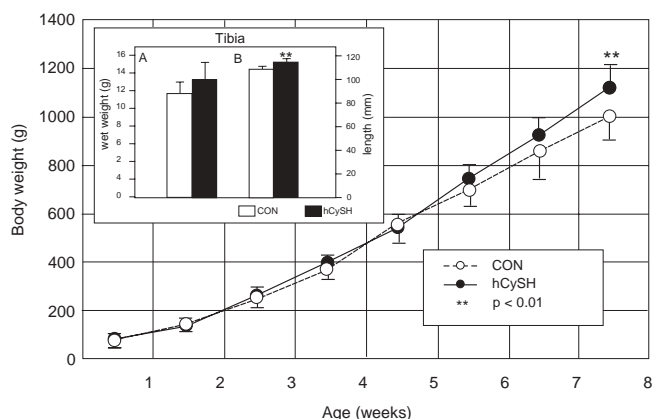


Figure 2
Growth curves (mean \pm SD of body weights) for control (CON) and hyperhomocysteinemic (hCySH) groups. hCySH-fed animals were significantly heavier at the end of the 8-week experiment (** $P < 0.01$). Inset: (A) tibial wet weight in grams; (B) length of tibia in millimeters (** $P < 0.01$).

icance (Figure 2 – Inset A); however, the positive difference for length (Figure 2 – Inset B) was significant ($P < 0.01$).

Table 2 gives biochemical data regarding sulfur amino acid and mineral metabolism for each group. Mean plasma total hCySH concentration in the experimental group was 8 times that of controls ($P < 0.0001$) and two other sulfur amino acids of interest, cystathionine and methionine, were also increased significantly ($P < 0.0001$ and $P < 0.001$, respectively). Cystathionine concentrations were elevated and there was a 30% increase in plasma inorganic sulfate (SO₄²⁻) ($P < 0.001$) in the experimental group under otherwise identical dietary sulfur conditions. However, there was no evidence for disturbance of glutathione metabolism, which is regulated independently of the transsulfuration pathway. There was also no difference in erythrocyte PLP levels. Methionine was increased by nearly 20%, indicating functional remethylation characteristic of CBS-deficient homocystinuria.

Plasma calcium and phosphate were normal in both groups (Table 2), and markers of bone formation – osteocalcin and bone specific ALP – did not vary significantly. Circulating IGF-1 was also not different, and values in both groups are comparable to chick data in the literature [35].

Table 2: Biochemical assessment of sulfur amino acid status, mineral metabolism, and bone formation.

Analyte	Group	
	Control	Experimental
Homocysteine (µmol/L)	43.8 ± 5.0	358 ± 58 ****
Methionine (µmol/L)	141 ± 9	175 ± 13 ***
Cystathionine (µmol/L)	39.8 ± 9.1	226 ± 20 ****
Total inorganic sulfate (mmol/L)	2.18 ± 0.44	3.09 ± 0.09 ***
Glutathione (µmol/L)	1141 ± 55	1066 ± 75
Pyridoxal-5'-phosphate (nmol/L)	162 ± 29	136 ± 46
Bone-specific alkaline phosphatase (IU/L)	2069 ± 317	2135 ± 370
Osteocalcin (µg/L)	1.58 ± 0.38	1.83 ± 0.63
IGF-I (µg/L)	16.9 ± 4.3	14.2 ± 3.4
Total calcium (mmol/L)	10.8 ± 0.2	10.7 ± 0.2
Phosphate (mmol/L)	7.3 ± 0.8	7.1 ± 0.9

****P < 0.0001 *** P < 0.001

Radiologic AP views of distal tibia from representative control (N) and hCySH-fed animals are seen in Figures 3A and 3B. It can be seen that there is better visualization of the trabeculae in control bone, while the hCySH-treated bone showed less radio-opacity. A well-defined radiolucency overlying the proximal metaphysis is seen in the hCySH-treated bone. Figures 3C and 3D are representative lateral views of whole tibia after loading to failure. At the proximal epiphysis of tibia are the *Tuberositas tibiae* and *Cristae tibiae* protuberances, to which the frequently ossified *Ligamenta recta patellae* are attached. At the distal epiphyses, the two joint ridges corresponding to the *Ossa tarsi* can be distinguished. The ovoid lucency visible in the metaphysis (black arrow) corresponds to an unmineralized, avascular collagen "plug", typical of chondrodysplasia seen on histological analysis (unpublished observation). In hyperhomocysteinemic animals (Figures 3B and 3D), the presence of multiple transverse lines of increased density at both proximal and distal ends (horizontal arrows) suggests more advanced ossification of the epiphyses. Increased cortical thickness is evident in both AP and LM views of hCySH-treated bone, particularly in the upper diaphyses. At the fracture site (Figure 3D), the jagged rupture pattern suggests that the bone from the hyperhomocysteinemic animal is more brittle than the control (Figure 3C).

As expected, AP outer (periosteal) diameters (*Y axis*) of the tibiae at mid-shaft were significantly greater than LM outer diameters (*X axis*) in both control ($P < 0.001$) and experimental ($P < 0.01$) groups (Figure 4A). The mean difference between the two axes was smaller in hCysH-fed animals. The outer AP diameter of their diaphyseal tibiae was significantly ($P < 0.01$) greater than in controls. Medullary cavity and cortical cross-sectional areas of hCySH-

treated bone were approximately 10% greater than those in controls (Figures 4B and 4C). Consequently, moments of inertia of hCySH-treated tibiae were greater, suggesting greater architectural efficiency of cross-sectional design (Figure 4D). However, none of these differences was statistically significant. The hCySH-treated bone looked bigger to the naked eye, a subjective observation confirmed by morphometric measurement (Figure 5). Differences in tibial diaphyseal profiles influenced overall shape of cortical bone in hyperhomocysteinemic animals, who displayed an abnormally eccentric and more elliptical medullary cavity. The thicker cortex on one side of hCySH-treated bone as compared to control was also noticeable on both AP and ML radiographs (Figures 3B and 3D).

Statistical analysis of biomechanical data also indicates that the hCySH-treated bone is stronger. Mean maximal load, stiffness and energy-at-failure were all greater than the values in controls (Figure 6). The increase for energy-at-failure was significant ($P < 0.01$). Analysis of covariance, correcting for morphometric differences, showed no significant differences in structural biomechanical properties when bone length and cortical thickness were included as covariates.

Table 3 describes the mineral and chemical properties of the hCySH-treated tibiae in comparison to controls. Ashing of diaphyseal tibial bone segments revealed that the proportion of mineral was not significantly different between groups. Infrared spectroscopy of hCySH-treated cortical bone showed no difference in terms of the mineral-to-matrix ratio when compared to controls. The collagen content of this bone, assessed by hydroxyproline content, was similar to controls. However, qualitative



Figure 3
Representative radiographs of the tibia at 8 weeks. Radiographs (A) and (B) show representative distal tibiae in anteroposterior (ap) position with growth plates still visible (horizontal bar = 7.5 mm). Bone from hCySH-treated animals (B) shows characteristic linear densities (white arrow) and spherical lucencies (black arrow) in cancellous bone in comparison to controls (A). Below are representative lateral (lat) radiologic views (vertical bar = 1 cm) of whole tibiae after loading to fracture. Here, a distinctive lucency (black arrow) is readily apparent in bone treated with hCySH (D) in comparison to control (C), but the trabecular elements of the secondary spongiosa seen in the anteroposterior radiographs are not as dramatic in these views. The metaphyseal lucency corresponds to an unmineralized avascular collagen 'plug' typical of chondrodysplasia. Note also the difference in rupture pattern.

changes in mineral composition were observed. The molar Ca^{2+}/PO_4^{3-} ratio was significantly higher ($P < 0.001$) in the experimental group and the CO_3^{3-}/PO_4^{3-} ratio, as revealed by FT-IR, was reduced ($P < 0.01$). X-ray diffraction analysis revealed no difference in the size and

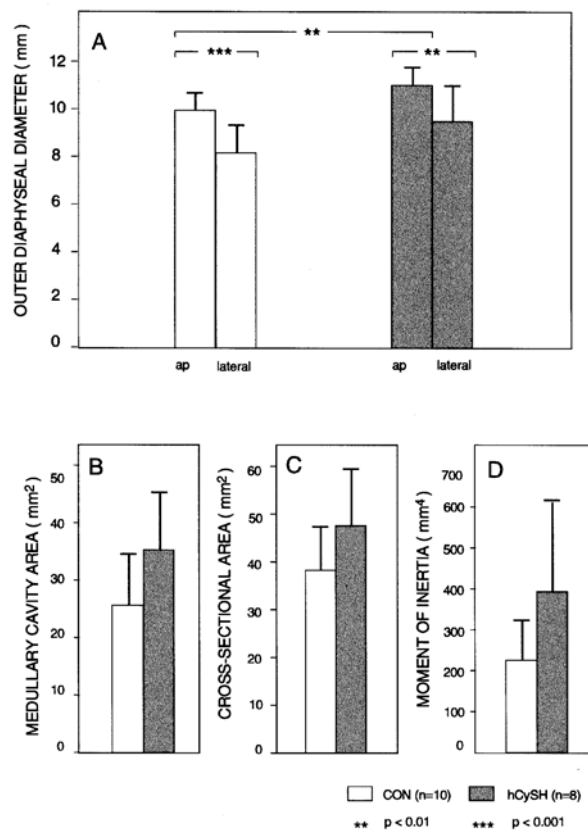


Figure 4
Geometric characteristics and structural properties of the tibia at mid-shaft. In panel (A) are shown the anteroposterior (ap) and lateral outer diaphyseal diameters (mean " SD). AP diameters are significantly greater than lateral diameters in both groups ($P < 0.01$). The difference between groups is also significant for AP diameters. Panels (B), (C), and (D) show medullary cavity area (mm^2), cross-sectional area (mm^2), and moment of inertia (mm^4), respectively. Dimensions for bone from hCySH-treated chicks was consistently greater.

symmetry of mineral crystals, as measured by line broadening (β_{002}).

Discussion

In the present study, the hCySH-rich diet administered to fast-growing chicks induces a bone disease bearing a striking similarity to early CBS-deficiency homocystinuria, including accelerated skeletal growth, epiphyseal growth plate lesions, and cortical bone chemical alterations [1-4,6]. The sulfur metabolite in the transsulfuration path-

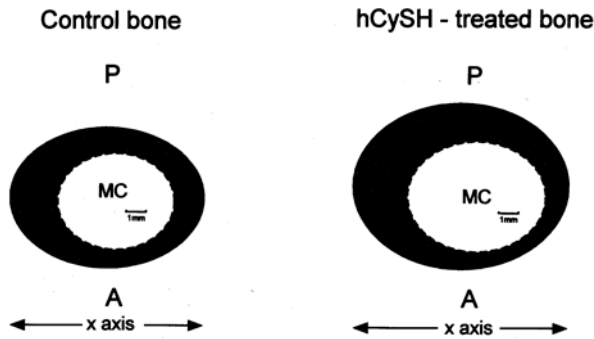


Figure 5
Mean mid-shaft tibial cross-sectional contours for control and homocysteine (hCySH)-treated animals. hCySH-treated cortical bone is asymmetric with an eccentric medullary cavity. Its greater thickness on one side of the X axis was also noticeable on radiographs (Figure. 4B). A: anterior cortex of tensile side; P: posterior cortex of compressive side; MC: medullary cavity; _____ periosteal cortical bone - - - - endosteal cortical bone. Bar = 1 mm.

way first associated with both accelerated skeletal growth and abnormal extracellular matrix was homocysteic acid [37,38], an oxidation product of homocysteine found in the urine of CBS-deficient patients [39]. In 1976, Clopath et al [38] demonstrated that homocysteic acid promoted growth of hypophysectomized rats, a finding associated with increased thickness of epiphyseal cartilage of the tibia and greater tail growth. We did not evaluate homocysteic acid directly, but we note that hCySH may be stimulatory *in vitro* when homocysteic acid is not [40], indicating the need for further studies to identify the key metabolite(s). Pteritz and others [6] postulate that a fibrillin defect may be central to the skeletal overgrowth phenotype, since the inherited fibrillin deficiency of Marfan syndrome induces connective tissue changes strikingly similar to that of CBS-deficiency homocystinuria. They have also been able to show that cysteine deficiency, which may occur in CBS-deficiency homocystinuria, can induce the fibrillin defect in culture [41], which has been reproduced in the developing chick [42]. Dietary cysteine deficiency in our model is unlikely because the chicks were fed a diet enriched in methionine (Table 1) and showed high circulating concentrations of the cysteine precursor, cystathionine, and the cysteine product, sulfate. However, the possibility that tissue insufficiency of cysteine (through competition with homocysteine [43], for example) may have specific hard tissue effects *in vivo* [44] could be tested in our model.

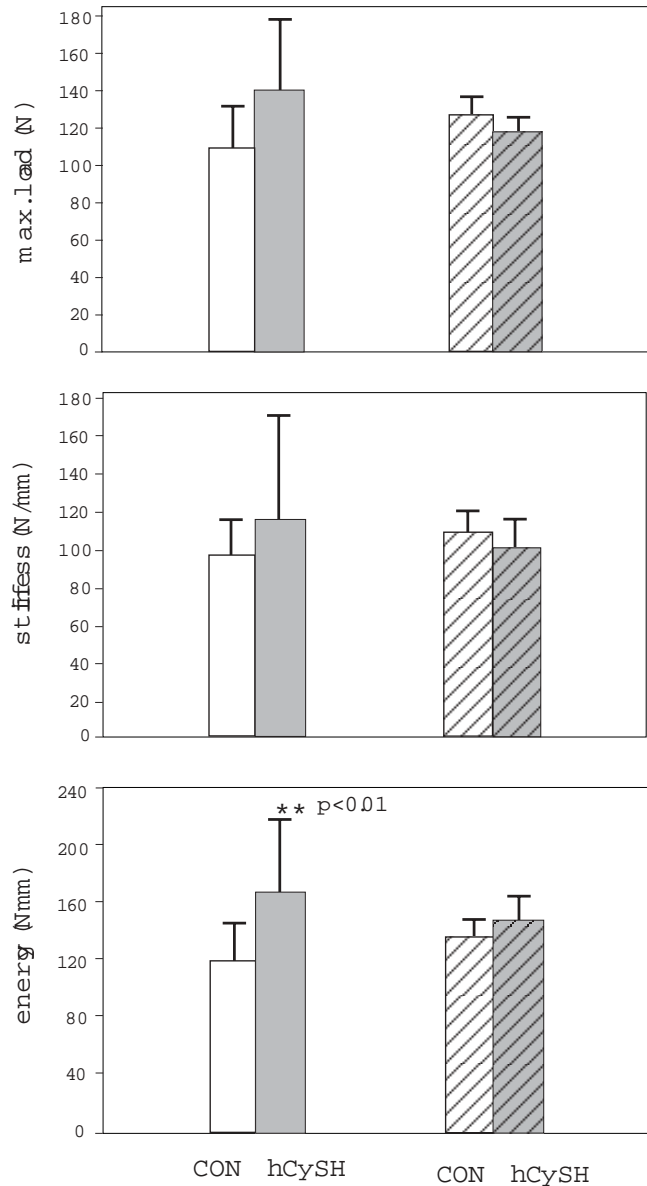


Figure 6
Biomechanical properties of the tibia. Top Panel – Maximum load (N); Middle Panel – Stiffness (N/mm); and Lower Panel – Energy at failure (N.mm). Unadjusted data (mean ± SD) for controls (CON) and hyperhomocysteinemic animals (hCySH) are shown by open and shaded bars, respectively. Bars with hatching show values statistically adjusted for length and cortical thickness by analysis of covariance.

The major skeletal changes noted in hyperhomocysteinemic animals in this study were the increased width and length of the tibia, features not present in the vitamin B₆ deficiency model [15]. However, cystathionine is the predominant sulfur amino acid elevated in that model [45],

Table 3: Chemical analyses of diaphyseal tibia

	Group	
	Control	Experimental
Ash (% of net weight)	61.2 ± 1.4	60.1 ± 1.4
Calcium:Phosphate (molar ratio)	1.79 ± 0.16	2.11 ± 0.15***
Hydroxyproline (µg/mg dry wt)	28 ± 3	29 ± 2
Mineral Matrix FT-IR peak area ratio	4.37 ± 0.35	4.43 ± 0.14
CO ₃ :PO ₄ FT-IR peak area ratio	0.0190 ± 0.001	0.0174 ± 0.001**
β ₀₀₂ (degrees)	0.531 ± 0.018	0.527 ± 0.024

*** P < 0.001 ** P < 0.01

not hCySH. In the present study, all three amino acids of the transsulfuration pathway – hCySH, cystathionine and methionine – were elevated (Table 2). Also unlike vitamin B₆ deficiency, qualitative alterations in the cortical bone mineral composition were observed. The bone carbonate to phosphate ratio was slightly but significantly ($P < 0.01$) decreased (Table 3), a finding associated with high turnover and remodeling rates [46]. The increased cross-sectional area of the medullary cavity (Figure 4B) may also reflect increased endosteal resorption.

The markers of bone formation we studied – osteocalcin and bone-specific ALP – were unchanged (Table 2), but these measures were recorded only at the end of the experiment when the bony abnormality had been established. Levels of IGF-1, a paracrine and autocrine stimulus of bone growth [47–51], were also normal, consistent with recent observations in human CBS deficiency [52]. The increased bone length we observed could be related to changes in the growth cartilage at the cellular level. Whether the proliferative zone of the ossification front or the number or size of hypertrophic chondrocytes is increased warrants further investigation.

The non-collagenous constituents of the epiphyseal matrix are likely important in the pathophysiology of accelerated bone growth. McCully demonstrated that addition of hCySH to culture medium of normal skin cells produced histological changes in proteoglycan structure similar to those found in CBS-deficient cell cultures, along with an increase in radiolabelled sulfate incorporation [53]. Although it was postulated that homocysteic acid may act as a sulfate source for phosphoadenosine phosphosulfate (PAPS), the substrate necessary for sulfoester and glycosaminoglycans synthesis, no direct confirmation of this concept has been reported [54]. The increased Ca/P ratio found on bone mineral analysis may parallel an elevation of extracellular calcium associated with a greater production of non-aggregated proteoglycans similar to those seen *in vitro* by others [53,55], but further study is

needed. Because of the strongly polyanionic nature of their sulfate and carboxylate groups, proteoglycans have a considerable capacity to form calcium complexes, which may serve as a readily accessible source of mineral for hydroxyapatite deposition [56]. In the osteochondrodystrophy induced by vitamin B₆ deficiency in the growing chick, connective tissue proteoglycans were found to be more extractable [45], consistent with the structural changes seen by light and electron microscopy in arteriosclerotic wall arteries [53]. Mineral abnormalities in a defective connective tissue matrix, particularly calcium, are also relevant to the role of hyperhomocysteinemia in arteriosclerosis [53,57].

Unlike osteogenesis imperfecta (OI) with its defective collagen synthesis [58,59], chemical changes and associated alterations in collagen morphology in this model [13] do not substantially alter biomechanical properties of long bone and the mineralization process itself, as assessed by the size and degree of symmetry in the mineral crystal analysis (β₀₀₂ line broadening) (Table 3). However, the increased moment of inertia of hyperhomocysteinemic bone (Figure 4D) and enhanced cortical thickness on one side (Figure 5) may compensate for abnormally asymmetric and weakened bone due to defective cross links [60] — hence, the lack of significant difference when size covariants such as length and cortical thickness were included.

This report presents a dietary chick model of severe hyperhomocysteinemia as a superior alternative to the CBS-knockout mouse [7] for study of connective tissue abnormalities. The homozygous knock-out mice display plasma hCySH concentrations forty times normal and succumb prematurely after suffering from growth retardation and marked liver disease, neither of which is typical of human CBS deficiency. The heterozygote knock-out animals have total homocysteine concentrations only twice that of wild-type, compared to a difference of more than 5-fold increase that is typical of human CBS deficiency [43] and seen in our experimental model.

Conclusions

In summary, this chick model demonstrates that changes in bone mineral composition, tibial cross-sectional contour, and radiological changes are induced by a hyperhomocysteinemic diet and associated with abnormal bone matrix. The hyperhomocysteinemia causes greater radial and longitudinal bone growth with more advanced ossification of epiphyses and greater architectural efficiency of the diaphyseal cross-sectional design, despite the collagen defect [13], chondrodysplastic cartilage, and the chemical abnormalities of bone. The cause of accelerated skeletal growth is an important subject for further study. Moreover, delineation of the factors maintaining normal biomechanical strength in osteopenic bone will be of direct relevance to the homocystinuric patient and the larger population at risk for idiopathic osteoporosis alike [61].

Competing interests

None declared.

Authors' contributions

Masse and Howell contributed equally to the study concept and design, preparation of the animal materials for analysis, and the basic biochemical measurements. Donovan performed assays of IGF-1 and Hauschka measured osteocalcin. Ziv did the biomechanical study and Boskey performed the bone chemistry measurements. Cole performed the sulfate and sulfur amino acid analyses and contributed to the statistical analysis and interpretation of the data as well as the primary editing of the final manuscript. All authors contributed to the written contents of this manuscript.

Acknowledgements

We are grateful to Dr. Jovan Evrovski (Dept. of Laboratory Medicine & Pathobiology, University of Toronto, Toronto ON Canada) for the sulfur amino acid and inorganic sulfate determinations, Dr. J.D. Mahuren (Fort Wayne State Developmental Center, Fort Wayne IN) for erythrocyte PLP determinations, Rhonda M Graves for bone chemistry, Dr. Mauricio Solano (Tufts University, Boston MA) for radiologic bone examination, Felix Soto for his technical assistance during animal care and dissections, and Dr. Loralie J. Langman (Dept. of Laboratory Medicine & Pathobiology, University of Toronto, Toronto ON Canada) for her editorial assistance in the preparation of this manuscript. This work was supported by grants from the Natural Sciences and Engineering Research Council of Canada (PGM, DECC), Dairy Farmers of Canada (DECC), NIH DE04141 and Cornell University Medical College (minority student grant) (ALB), the GRECC (Veterans Administration Medical Center, Miami) (DSH) and USDA/NRICGP grant 95-37200-1703 (JDM), and the Heart & Stroke Foundation of Ontario grants B-3584 and T4340 (DECC).

References

- Mudd SH, Levy HL and Kraus JP **Disorders of transsulfuration**. In: *The metabolic and molecular bases of inherited disease* (Edited by: Scriver CR, Beaudet AL, Sly WS, Valle D) New York: McGraw Hill Inc. 2001, 2007-2056
- Schedewie H, Willich E, Grobe H, Schmidt H and Muller KM **Skeletal findings in homocystinuria: A collaborative study**. *Pediatr Radiol* 1973, **1**:12-23
- Brenton DP **Skeletal abnormalities in homocystinuria**. *Postgrad Med J* 1977, **53**:488-494
- Mudd SH, Skovby F, Levy HL, Pettigrew KD, Wilcken B and Pyeritz RE **The natural history of homocystinuria due to cystathionine β -synthase deficiency**. *Am J Hum Genet* 1985, **37**:1-31
- Parrot F, Redonnet-Vernhet I, Lacombe D and Gin H **Osteoporosis in late-diagnosed adult homocystinuric patients**. *J Inherit Metab Dis* 2000, **23**:338-340
- Pyeritz RE **Homocystinuria**. In: *McKusick's heritable disorders of connective tissue* (Edited by: Beighton P) St. Louis: Mosby 1993, 137-178
- Watanabe M, Osada J, Aratani Y, Kluckman K, Reddick R and Malinow MR **Mice deficient in cystathionine β -synthase: Animal models for mild and severe homocyst(e)inemia**. *Proc Natl Acad Sci U S A* 1995, **92**:1585-1589
- Wilmarth KR and Froines JR **In vitro and in vivo inhibition of lysyl oxidase by aminopropionitriles**. *J Toxicol Environ Health* 1992, **37**:411-423
- Levene CI **The hydrating effect of lathyrogenic compounds on chick-embryo cartilage in vivo**. *Biochem J* 1966, **101**:441-447
- Orth MW, Martinez DA, Cook ME and Vailas AC **Nonreducible crosslink formation in tibial dyschondroplastic growth plate cartilage from broiler chicks fed homocysteine**. *Biochem Biophys Res Commun* 1991, **179**:1582-1586
- Orth MW, Bai Y, Zeytun IH and Cook ME **Excess levels of cysteine and homocysteine induce tibial dyschondroplasia in broiler chicks**. *J Nutr* 1992, **122**:482-487
- Orth MW, Leach RM, Vailas AC and Cook ME **Non-reducible collagen cross-linking in cartilage from broiler chickens with tibial dyschondroplasia**. *Avian Dis* 1994, **38**:44-49
- Masse PG, Colombo VE, Gerber F, Howell DS and Weiser H **Morphological abnormalities in vitamin B₆ deficient tarsometatarsal chick cartilage**. *Scan Microscopy* 1990, **4**:667-674
- Masse PG, Pritzker KPH, Mendes MG, Boskey AL and Weiser H **Vitamin B₆ deficiency experimentally-induced bone and joint disorder: microscopic, radiographic and biochemical evidence**. *Br J Nutr* 1994, **71**:919-932
- Masse PG, Rinnac CM, Yamauchi M, Coburn SP, Rucker RB and Howell DS **Pyridoxine deficiency affects biomechanical properties of chick tibial bone**. *Bone* 1996, **18**:567-574
- Masse PG, Yamauchi M, Mahuren JD, Coburn SP, Muniz OE and Howell DS **Connective tissue integrity is lost in vitamin B-6-deficient chicks**. *J Nutr* 1995, **125**:26-34
- Burstein AH, Zika JM, Heiple KG and Klein L **Contribution of collagen and mineral to the elastic-plastic properties of bone**. *J Bone Joint Surg [Am]* 1975, **57**:956-961
- Spengler DM, Baylink DJ and Rosenquist JB **Effect of beta-aminopropionitrile on bone mechanical properties**. *J Bone Joint Surg [Am]* 1977, **59**:670-672
- Reddi AH and Sullivan NE **Inhibition of mineralization by experimental lathyrisms during matrix-induced endochondral bone differentiation**. *Proc Soc Exp Biol Med* 1979, **162**:445-448
- Sandhu HS and Jande SS **Effects of beta-aminopropionitrile on formation and mineralization of rat bone matrix**. *Calcif Tissue Int* 1982, **34**:80-85
- Gerstenfeld LC, Riva A, Hodgens K, Eyre DR and Landis WJ **Post-translational control of collagen fibrillogenesis in mineralizing cultures of chick osteoblasts**. *J Bone Miner Res* 1993, **8**:1031-1043
- Mahuren JD and Coburn SP **B-6 vitamers: cation-exchange HPLC**. *J Nutr Biochem* 1990, **1**:659-663
- Evrovski J, Callaghan M and Cole DEC **Determination of homocysteine by HPLC with pulsed integrated amperometry**. *Clin Chem* 1995, **41**:757-758
- Cole DEC and Scriver CR **Microassay of inorganic sulfate in biological fluids by controlled flow anion chromatography**. *J Chromatogr* 1981, **225**:359-367
- Cole DEC and Evrovski J **Quantitation of sulfate and thiosulfate in clinical samples by ion chromatography**. *J Chromatogr A* 1997, **789**:221-232
- Borgers ME and Thoné F **The inhibition of alkaline phosphatase by L-bromotetramisole**. *Histochem* 1975, **44**:277-280
- Hauschka PV, Frenkel J, DeMuth R and Gundberg CM **Presence of osteocalcin and related higher molecular weight 4-carboxyglutamic acid-containing proteins in developing bone**. *J Biol Chem* 1983, **258**:176-182

28. Gundberg CM, Hauschka PV, Lian JB and Gallop PM **Osteocalcin: isolation, characterization, and detection.** *Methods Enzymol* 1984, **107**:516-544
29. Zhao X, Unterman TG and Donovan SM **Human growth hormone but not human insulin-like growth factor-I enhances recovery from neonatal malnutrition in rats.** *J Nutr* 1995, **125**:1316-1327
30. Church LE and Johnson LC **Growth of long bones in the chicken: Rates of growth in length and diameter of humerus, tibia, and metatarsus.** *Am J Anat* 1964, **114**:521-538
31. Bak B, Jorgensen PH and Andreassen TT **Increased mechanical strength of healing rat tibial fractures treated with biosynthetic human growth hormone.** *Bone* 1990, **11**:233-239
32. Ferretti JL, Spiaggi EP, Capozza R, Cointry G and Zanchetta JR **Interrelationships between geometric and mechanical properties of long bones from three rodent species with very different biomass: phylogenetic implications.** *J Bone Miner Res* 1992, **7 Suppl 2**:S433-S435
33. Ferretti JL, Capozza RF, Mondelo N and Zanchetta JR **Interrelationships between densitometric, geometric, and mechanical properties of rat femora: inferences concerning mechanical regulation of bone modeling.** *J Bone Miner Res* 1993, **8**:1389-1396
34. Han SM, Szarzanowicz TE and Ziv I **Effect of ovariectomy and calcium deficiency on the ultrasound velocity, mineral density and strength in the rat femur.** *Clin Biomechanics* 1998, **13**:480-484
35. Klug HP and Alexander LE **X-ray diffraction procedures for polycrystalline and amorphous materials.** New York: Wiley 1974,
36. Hutterer F and Singer EG **A modified method for hydroxyproline determination.** *Anal Chem* 1970, **32**:556-558
37. McCully KS **Macromolecular basis for homocystein-induced changes in proteoglycan structure in growth and arteriosclerosis.** *Am J Pathol* 1972, **66**:83-96
38. Clopath P, Smith VC and McCully KS **Growth promotion by homocysteic acid.** *Science* 1976, **192**:372-374
39. Lubec B, Fang-Kircher S, Lubec T, Blom HJ and Boers GH **Evidence for McKusick's hypothesis of deficient collagen cross-linking in patients with homocystinuria.** *Biochim Biophys Acta* 1996, **1315**:159-162
40. Fritzer-Szekeres M, Blom HJ, Boers GH, Szekeres T and Lubec B **Growth promotion by homocysteine but not by homocysteic acid: a role for excessive growth in homocystinuria or proliferation in hyperhomocysteinemia?** *Biochim Biophys Acta* 1998, **1407**:1-6
41. Majors AK and Pyeritz RE **A deficiency of cysteine impairs fibrillin-1 deposition: implications for the pathogenesis of cystathionine beta-synthase deficiency.** *Mol Genet Metab* 2000, **70**:252-260
42. Hill CH, Mecham R and Starcher B **Fibrillin-2 defects impair elastic fiber assembly in a homocysteinemic chick model.** *J Nutr* 2002, **132**:2143-2150
43. Hargreaves IP, Lee PJ and Briddon A **Homocysteine and cysteine - albumin binding in homocystinuria: assessment of cysteine status and implications for glutathione synthesis?** *Amino Acids* 2002, **22**:109-118
44. Maclean KN, Gaustadnes M, Oliveriusova J, Janosik M, Kraus E and Kozich V **High homocysteine and thrombosis without connective tissue disorders are associated with a novel class of cystathionine beta-synthase (CBS) mutations.** *Hum Mutat* 2002, **19**:641-655
45. Masse PG, Ziv I, Cole DE, Mahuren JD, Donovan SM and Yamauchi M **A cartilage matrix deficiency experimentally induced by vitamin B6 deficiency.** *Proc Soc Exp Biol Med* 1998, **217**:97-103
46. Rey C, Beshah K, Griffin R and Glimcher MJ **Structural studies of the mineral phase of calcifying cartilage.** *J Bone Miner Res* 1991, **6**:515-525
47. Schwander JC, Hauri C, Zapf J and Froesch ER **Synthesis and secretion of insulin-like growth factor and its binding protein by the perfused rat liver: dependence on growth hormone status.** *Endocrinology* 1983, **113**:297-305
48. Canalis E, McCarthy T and Centrella M **Growth factors and the regulation of bone remodeling.** *J Clin Invest* 1988, **81**:277-281
49. Isaksson OG, Nilsson A, Isgaard J and Lindahl A **Cartilage as a target tissue for growth hormone and insulin-like growth factor I.** *Acta Paediatr Scand Suppl* 1990, **367**:137-141
50. Spencer EM, Liu CC, Si EC and Howard GA **In vivo actions of insulin-like growth factor-I (IGF-I) on bone formation and resorption in rats.** *Bone* 1991, **12**:21-26
51. Johansson AG, Lindh E and Ljunghall S **Insulin-like growth factor I stimulates bone turnover in osteoporosis [letter].** *Lancet* 1992, **339**:1619
52. Topaloglu AK, Sansaricq C and Snyderman SE **Influence of Metabolic Control on Growth in Homocystinuria due to Cystathionine B-Synthase Deficiency.** *Pediatr Res* 2001, **49**:796-798
53. McCully KS **Importance of homocysteine-induced abnormalities of proteoglycan structure in arteriosclerosis.** *Am J Pathol* 1970, **59**:181-194
54. Cole DEC and Evrovski J **The clinical chemistry of inorganic sulfate.** *Crit Rev Clin Lab Sci* 2000, **37**:299-344
55. Modis L, Hadhazy C, Laszlo MB, Kostenszky KS and Foldes I **Proteoglycan biosynthesis is stimulated by D-penicillamine in chondrifying high density cell cultures.** *Exp Pathol* 1988, **35**:159-176
56. Hunter GK **In vitro studies on matrix-mediated mineralization.** In *Bone metabolism and mineralization* (Edited by: Hall BK) Boca Raton: CRC Press 1992, 225-247
57. Rolland PH, Friggi A, Barlatier A, Piquet P, Latrille V and Faye MMGJ **Hyperhomocysteinemia-induced vascular damage in the minipig. Captopril-hydrochlorothiazide combination prevents elastic alterations.** *Circulation* 1995, **91**:1161-1174
58. Pereira RF, Hume EL, Halford KVV and Prockop DJ **Bone fragility in transgenic mice expressing a mutated gene for type I procollagen (COL1A1) parallels the age-dependent phenotype of human osteogenesis imperfecta.** *J Bone Miner Res* 1995, **10**:1837-1843
59. Camacho NP, Hou L, Toledano TR, Ilg WA, Brayton CF and Raggio CL **The material basis for reduced mechanical properties in oim mice bones.** *J Bone Miner Res* 1999, **14**:264-272
60. Cordey J, Schneider M, Belendez C, Ziegler WJ, Rahn BA and Perren SM **Effect of bone size, not density, on the stiffness of the proximal part of normal and osteoporotic human femora.** *J Bone Miner Res* 1992, **7 Suppl 2**:S437-S444
61. van der Meulen MC, Jepsen KJ and Mikic B **Understanding bone strength: size isn't everything.** *Bone* 2001, **29**:101-104

Pre-publication history

The pre-publication history for this paper can be accessed here:

<http://www.biomedcentral.com/1471-2474/4/2/prepub>

Publish with **BioMed Central** and every scientist can read your work free of charge

"BioMed Central will be the most significant development for disseminating the results of biomedical research in our lifetime."

Sir Paul Nurse, Cancer Research UK

Your research papers will be:

- available free of charge to the entire biomedical community
- peer reviewed and published immediately upon acceptance
- cited in PubMed and archived on PubMed Central
- yours — you keep the copyright

Submit your manuscript here:
http://www.biomedcentral.com/info/publishing_adv.asp

